Temperature and pressure effects on the product distribution of PTFE pyrolysis by means of qualitative, in-line FTIR analysis

Miss Anya Bezuidenhoudt*

*Corresponding author. Tel.: +27767288158;

E-mail address: abezuidenhoudt@hotmail.com

Mr Paul W Sonnendecker

E-mail address: paul.sonnendecker@up.ac.za

Prof Philip L Crouse

E-mail address: philip.crouse@up.ac.za

Department of Chemical Engineering
Faculty of Engineering, Built Environment & IT
University of Pretoria
Lynnwood road
Hatfield
Pretoria
South Africa
0002

Abstract

The results of the depolymerisation of PTFE under steady operating conditions in a semi-automated, continuous depolymerisation system are presented. The influence of temperature and pressure on the selectivity of the three main products of depolymerisation (tetrafluoroethylene (TFE), hexafluoropropylene (HFP), and octafluorocyclobutane (OFCB)) was investigated via qualitative in-line FTIR analysis. No carrier gas was used, with the PTFE feed rate and experimental run time kept constant. The temperature and pressure ranges investigated were: 650 °C — 750 °C and <10 kPa — 40 kPa. The optimum operating conditions to maximise the three main products were determined using response surface methodology following a three-level face centered composite design. A TFE mole fraction of 0.95 and higher was achieved at operating conditions of ± 675 °C and < 10 kPa. HFP mole fractions of 0.19 and higher were achieved within the operating range of 744 °C to 750 °C and 32 kPa up to 40 kPa. At operating conditions of 750 °C and 40 kPa, OFCB fractions of 0.5 – 0.55 were achieved. The OFCB and HFP mole fractions achieved differed from those previously mentioned in the literature. Analysis of the determined product specific kinetics indicates that the predominant HFP production pathway at low residence times (< 3 s) is via the reaction of TFE with difluorocarbenes. At higher residence times the dominant reaction pathway is the dissociation OFCB.

Keywords: PTFE depolymerisation; tetrafluoroethylene; in-line FTIR; regression analysis, product-specific analysis

1 Introduction

Fluoropolymers are important synthetic materials in science and industry and are used to meet a variety of severe specifications required by modern engineering. The most important of all of the industrial fluoropolymers is polytetrafluoroethylene (PTFE) due to its wide range of unique and extraordinary characteristics. Due to the non-melt-processability of PTFE resin, a large amount of waste is generated annually, most of which is either incinerated, landfilled or ground up and ram extruded to produce lower quality tubes and profiles [1][2]. These destructive or re-use methods pose economic and environmental issues, particularly when considering the evolution of extremely toxic gases (*eg* perfluoroisobutylene (PFIB)) during the incineration of PTFE. In recent years, methods of PTFE recycling have been investigated, with the main focus on the thermal decomposition of PTFE. This process produces high-value monomers, which include tetrafluoroethylene (TFE), hexafluoropropylene (HFP) and octafluorocyclobutane (OFCB) [3]. Due to the transport and handling restrictions and difficulties of TFE, it has become commercially unavailable, leading to the requirement of safe, on-site production methods [4]. Since TFE is produced during the decomposition of PTFE, waste PTFE can in principle be used to produce new, high molecular weight PTFE in a multi-unit operation process.

The effects of temperature and pressure on the product distribution achieved during continuous PTFE depolymerisation have been reported numerous times in the literature [1 – 2] [5 – 7]. Even though the overall effects of these two variables seem to stay the same, experimental results achieved at the University of Pretoria indicate that the exact distribution of the three main products (TFE, HFP, and OFCB) appear to be system specific. Meissner [6] and van der Walt [2]performed in-depth studies into the temperature and pressure effects on the product distribution and recommended the

optimum operating conditions to optimise the three main products (TFE, HFP, and OFCB).

The main aim of this investigation was to determine the temperature and pressure effects on the selectivity of TFE, HFP, and OFCB for this particular system. If PTFE depolymerisation were to be used as a recycle method it would be beneficial to determine the operating conditions that would favour the production of single and two component systems. Since there is a small difference in the relative volatilities of HFP and OFCB, it would be advantageous to produce two component systems of TFE with either HFP or OFCB maximised. These operating conditions were determined statistically via a qualitative in-line FTIR analysis method developed in-house. The product specific kinetics of the system were also determined to achieve an in-depth analysis of the depolymerisation process.

2 Depolymerisation mechanism

The mechanism of PTFE depolymerisation has been of interest since its discovery. Lewis [3] first proposed the unzipping or free-radical chain mechanism. Morisaki [8] proposed an elaborate PTFE depolymerisation mechanism which includes the formation pathways of most of the common depolymerisation products. Meissner [6] proposed a similar mechanism. In both Morisaki [8] and Meissner's [6] mechanisms, two HFP formation reactions were proposed. According to Meissner [6], the decomposition of OFCB is the most likely HFP production pathway. According to van der Walt [2], another depolymerisation mechanism may be present at high temperatures (700 °C to 900 °C), which involves the polymer chain randomly breaking into fragments. From the literature cited, it can be concluded that the process of PTFE depolymerisation may occur via two possible mechanisms which are temperature dependent. The depolymerisation process can be divided up into five steps: Initiation, primary product formation, secondary and tertiary reaction steps and

finally the recombination step. The main proposed mechanisms for each step is summarised below, including all of the possible pathways of product formation.

1. *Initiation*

$$— (CF_2 - CF_2)_n — \rightarrow R_a — CF_2 \bullet + \bullet CF_2 — R_b \quad (1)$$

2. *Primary product formation*

Difluorocarbene $$R_a — CF_2 \bullet \rightarrow \bullet\bullet CF_2 + \bullet CF_2 — R_b \quad (2)$$

TFE Formation $$2 \bullet\bullet CF_2 \rightarrow CF_2 = CF_2 \quad (3)$$

3. *Secondary product formation*

OFCB formation $$2CF_2 = CF_2 \rightarrow \bullet CF_2 — CF_2 — CF_2 — CF_2 \bullet \rightarrow OFCB \quad (4)$$

HFP formation $$CF_2 = CF_2 + \bullet\bullet CF_2 \rightarrow CF_3 — CF = CF_2 \quad (5)$$

4. *Tertiary product formation*

HFP formation $$OFCB \rightarrow CF_3 — CF = CF_2 + \bullet\bullet CF_2 \quad (6)$$

1-OFB or PFIB formation $$CF_3 — CF = CF_2 + \bullet\bullet CF_2 \rightarrow CF_3CF_2CF = CF_2 \; or \; (CF_3)_2C — CF_2 \quad (7)$$

5. *Recombination step*

$$R_a — CF_2 \bullet + \bullet CF_2 — R_b \rightarrow R_a — CF_2 — CF_2 — R_b \quad (8)$$

3 Experimental

3.1 Raw material

Teflon® PTFE 807N was procured from DuPont (now known as Chemours) to be used as raw material for this investigation. The general material properties for Teflon® PTFE 807N are listed in Table 1.

Table 1: DuPont Teflon® PTFE 807N physical properties (DuPont, *sa*)

Average particle diameter	µm	600
Standard specific gravity		2.156
Bulk density	g·cm^{-3}	0.95
Melting peaks		
Initial	°C	344
Second	°C	327

3.2 Apparatus and operation

PTFE depolymerisation was achieved in the semi-automated depolymerisation system depicted in Figure 1. The system was remotely controlled and monitored by software written in National Instruments ™ LabVIEW Full Development Suite 2015. The system consists of a stainless steel pipe reactor 381 mm in length, with an internal diameter of 77.92 mm. The reactor was flanged using a Viton seal. In the top flange, a one-inch bore pipe connected the reactor to a ball valve and another one-inch bore pipe connected the ball valve to a screw feeder. The screw was operated using a reversible, geared AC induction motor. A variable frequency drive (VFD) was used to control the motor speed. The reactor was heated using a resistive furnace. The reactor temperature was monitored at three places; one thermocouple at the bottom of the reactor, one thermocouple halfway up the reactor and the last thermocouple was inserted in the reactor outlet tube. Glass wool was inserted in the reactor outlet to prevent any debris from entering the rest of the system. The product gas evolved during depolymerisation was pumped to a holding cylinder using a diaphragm pump. The system pressure during operation was controlled manually by restricting the product gas flow using valve V5.

No carrier gas was used. The Teflon® PTFE 807N feed rate was kept constant at 11 $g \cdot min^{-1}$ ($\pm$ 0.31 $g \cdot min^{-1}$) by setting the VFD frequency to 30 Hz. The experimental run time was 15 min. The first 5 min was used to pressurise the system and to allow the system to reach steady state.

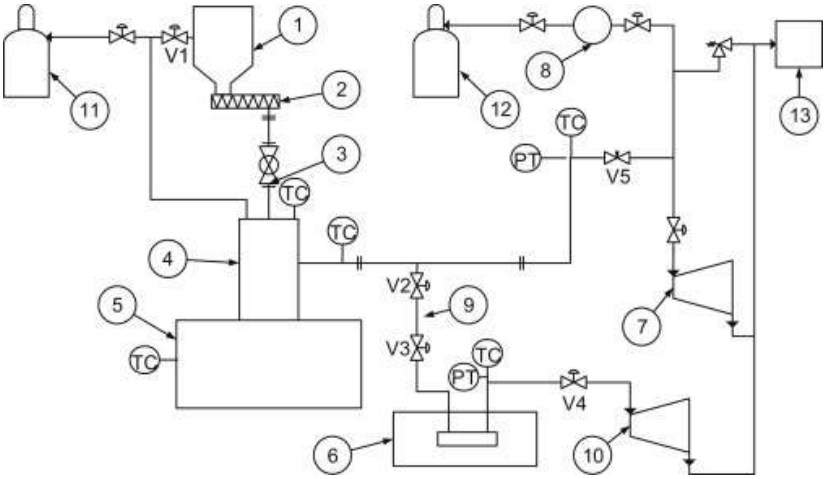

Figure 1 Schematic layout of the continuous depolymerisation setup: (1) hopper, (2) screw feeder, (3) ball valve, (4) pyrolysis reactor, (5) furnace, (6) FTIR spectrometer, (7 and 10) vacuum pump, (8) diaphragm pump, (9) sampling tube, (11) inert gas cylinder, (12) holding cylinder, (13) vent.

3.3 Experimental design

The influence of temperature and pressure on the selectivity of TFE, HFP, and OFCB, was investigated using Response Surface Methodology (RSM) with temperature and pressure selected as input variables following a Face Centered Composite (CCF) design (NIST/SEMATECH, 2012). Meissner [6] and van der Walt [2] confirm that the response surface for each of the depolymerisation products is anything but linear. To incorporate this finding, a three-level full factorial design was followed. All of the experimental points were repeated twice to determine the stability of the system. The three level values for each of the two factors are indicated in Table 2. In total 27 experiments were performed.

Table 2: The levels of the two examined factors.

Level	Coded value	Temperature (°C)	Pressure (kPa)
	X_i	x_1	x_2
High	1	750	40
Centre point	0	700	20
Low	-1	650	< 10

3.4 Data analysis

3.4.1 FTIR spectral analysis method

FTIR spectra were generated at intervals of 15 s using Perkin Elmer ® Spectrum Timebase™ software. Spectra were measured between 3000 and 1000 cm^{-1} on gas samples in a gas cell with CaF_2 windows and a path length of 15 mm. The instrument resolution was set on 4 cm^{-1} with a data interval of 1 cm^{-1}. The instrument is fitted with a MIR source, optical KBr beamsplitter and windows and a $LiTaO_3$ source.

The generated spectra were smoothed and baseline corrected by means of the asymmetric least squares method proposed by Eilers [9]. Spectra were fitted with known spectra from the individual components generated in the lab and solved by means of a Levenberg-Marquardt non-linear solver. The qualitative analysis was determined from Beer's law and previously generated concentration versus absorbance curves generated in the lab.

3.4.2 Statistical analysis

The effects of each of the independent factors on the response values of the process were estimated using the general quadratic equation represented by Equation (9). This equation comprises a constant, two linear components, two square components, and the cross product representing the interaction effects of temperature and pressure on the response surface. The response functions of the system were described by the following: Y_1 — TFE, Y_2 — HFP and Y_3 — OFCB.

To simplify calculations and determine the significance of each of the variables in Equation (9), the factor values were coded (see Table 2) using Equations (10), (11) and (12), with x_i as the actual factor value, x_H as the "high" factor value and x_L the "low" factor value. The coded experimental design matrix is given in Table 3.

$$Y_i = \beta_0 + \beta_1 X_1 + \beta_2 X_2 + \beta_3 X_1 X_2 + \beta_4 X_1^2 + \beta_5 X_2^2 \quad (9)$$

$$X_i = \frac{(x_i - a)}{b} \quad (10)$$

$$a = \frac{(x_H + x_L)}{2} \quad (11)$$

$$b = \frac{(x_H - x_L)}{2} \quad (12)$$

After determining the initial response functions for each of the response values, the statistical significance of each of the variables was determined by analysing their F and P - values as well as by comparing the magnitudes of the individual coefficients.

The response values used in the regression analysis were determined by calculating the mean product-specific mole fraction produced during steady state operation at a specific operating temperature and pressure (see Table 3).

Table 3: The design matrix of the experiments in coded form and the experimental values of response functions $Y_1 - Y_3$.

Run number	X_1	X_2	Y_1	Y_2	Y_3
			Mole fraction		
1	-1	-1	0.968	0.028	0.0018
2	-1	1	0.307	0.156	0.532
3	1	-1	0.904	0.065	0.028
4	1	1	0.218	0.225	0.546
5	0	-1	0.950	0.044	0.005
6	0	1	0.319	0.157	0.513
7	-1	0	0.598	0.106	0.295
8	1	0	0.284	0.308	0.388
9	0	0	0.633	0.110	0.255
10	0	0	0.533	0.102	0.360
11	0	0	0.641	0.094	0.263
12	-1	-1	0.903	0.041	0.053
13	-1	1	0.421	0.135	0.437
14	1	-1	0.666	0.111	0.208
15	1	1	0.245	0.195	0.550
16	0	-1	0.934	0.044	0.022
17	0	1	0.306	0.146	0.544
18	-1	0	0.594	0.132	0.261
19	1	0	0.408	0.148	0.439
20	-1	-1	0.946	0.035	0.017
21	-1	1	0.309	0.134	0.549
22	1	-1	0.739	0.092	0.161
23	1	1	0.213	0.246	0.529
24	0	-1	0.873	0.055	0.067
25	0	1	0.429	0.144	0.422
26	-1	0	0.605	0.115	0.274
27	1	0	0.476	0.135	0.383

3.4.3 Residence time estimation

Assuming the universal gas law holds, the residence time of the gas in the reactor at a constant temperature, constant PTFE flow rate, and constant reactor volume is only dependent on the system pressure. An increase in system pressure leads to a proportional increase in residence time since the reactor volume is constant. As a result, the TFE, OFCB, and HFP mole percentages at the three system pressures (< 10 kPa, 20 kPa, and 40 kPa) can be plotted against residence time for each temperature. It was also assumed that the depolymerisation reaction and side reactions only occur in the reactor and that the reactions stop once the gas has left the reactor. The residence time can be estimated using Equation (13):

$$\tau = \frac{P \cdot V_{Reactor}}{\dot{n}_{system} \cdot R \cdot T} \quad (13)$$

In the equation, $\dot{n}_{system}$ is the number of moles of the gas produced per unit time at a specific reactor pressure and temperature, R, is the universal gas constant, T, is the actual reactor temperature, P, is the corresponding reactor pressure and $V_{Reactor}$, is the reactor volume (1.36×10^{-3} m^3). By using the average mole percentage of TFE, HFP, and OFCB produced at a specific reactor pressure and temperature, and the assumption that 0.183 g PTFE·s^{-1} is fed, the average moles of the gas is calculated using equation (14).

$$n_{system} = \frac{0.184}{\sum_i (n_{fraction_i}) \cdot (MM_i)} \quad (14)$$

4 Results and discussion

4.1 Statistical analysis of the tetrafluoroethylene yield

Analysis of the P-values, t-statistic values and the Upper and Lower 95 % confidence interval values of the TFE initial response function indicated that the interaction variable ($\beta_3 X_1 X_2$) was statistically insignificant. No significant change in the R^2 and adjusted R^2 values were

noticed upon removal of the interaction variable (see Table 4). Hence, the TFE response surface (Figure 2) could be predicted using Equation (15). The data in Figure 2 was validated by comparing the contour plots to the actual TFE mole fractions measured (Table 3). As seen from the data in Figure 2, the contour plots are reasonably accurate, accept for the data points at 750 °C. The generated contour plots can be improved by increasing the number of experimental data points used to calculate equation (15), however, the equation can still be used to produce realistic predictions of the TFE mole fraction.

Table 4: Regression analysis comparison for the TFE response surface.

	Initial regression analysis with $\beta_3 X_1 X_2$ included	**Regression analysis with $\beta_3 X_1 X_2$ excluded**
R^2	0.961	0.960
Adjusted R^2	0.951	0.953
Significance F	4.57E-14	4.7E-15
Standard error	0.057	0.056

$$Y_1 = 0.5927 - 0.0642X_1 - 0.333X_2 - 0.0823X_1^2 + 0.1028X_2^2 \quad (15)$$

TFE production was more sensitive to changes in pressure than temperature. To compare the results of this investigation to those of Meissner [6], contour plots were produced using the response surface equations of Meissner [6]. The nitrogen flow rate and PTFE feeding rate values used in the equations were 0 $dm^3 \cdot h^{-1}$ and 11 $g \cdot min^{-1}$, respectively. From these plots (Figure 3 and Figure 4) it is clear that the TFE concentration decreased with an increase in temperature and pressure which coincides with the data depicted in Figure 2.

The optimum operating conditions to optimise the TFE mole fraction for this system were determined to be ± 675 °C and < 10 kPa. At these conditions, TFE mole fractions of ±95 % were achieved. These operating conditions coincided with those proposed by van der Walt [2] and the data predicted by Meissner [6].

The difference in the pressure and temperature dependence of TFE between Figure 2 and Figure 3 could be attributed to the residence time of the gas in the vertical reactor of Meissner [6] and is discussed further in section 4.3.

Spontaneous polymerisation of TFE was noticed, with PTFE dust settling on the walls of the piping throughout the system. This could be prevented by lining the piping with any one of the inhibitors mentioned in Drobny [10]. However, caution should be taken as most of the auto-ignition temperatures of these inhibitors are well below the standard operating temperatures of the depolymerisation reactor. Therefore, the piping system further down the line could be lined with an inhibitor but should be avoided close to the reactor.

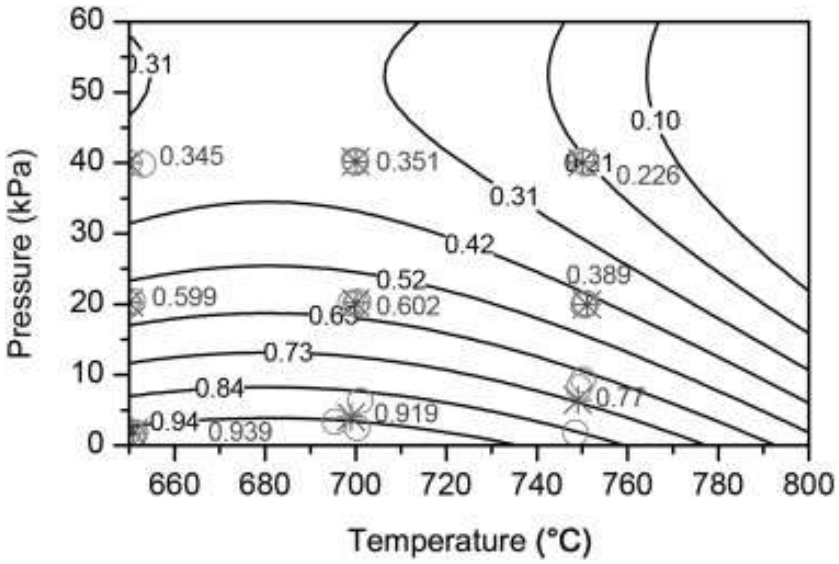

Figure 2 The contour plot of the influence of temperature and pressure on the fractional distribution of TFE as calculated using equation 15. Data validation was achieved by including the actual experimental data points (O) and the averages calculated for each set which is denoted by a star.

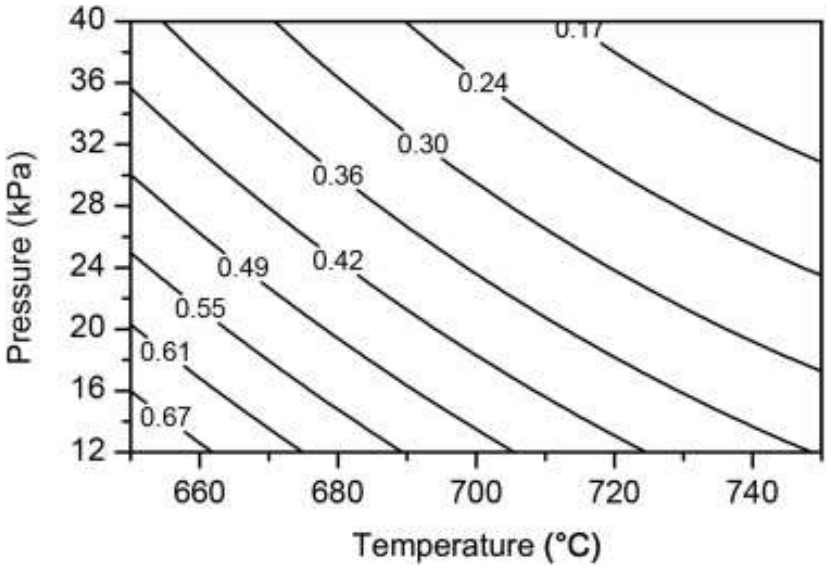

Figure 3 The effect of temperature and pressure on the TFE mole fraction as determined by Meissner [6] in the first section of the horizontal reactor. The contour plot was generated using the response surface equations of Meissner [6] for TFE (Y_2).

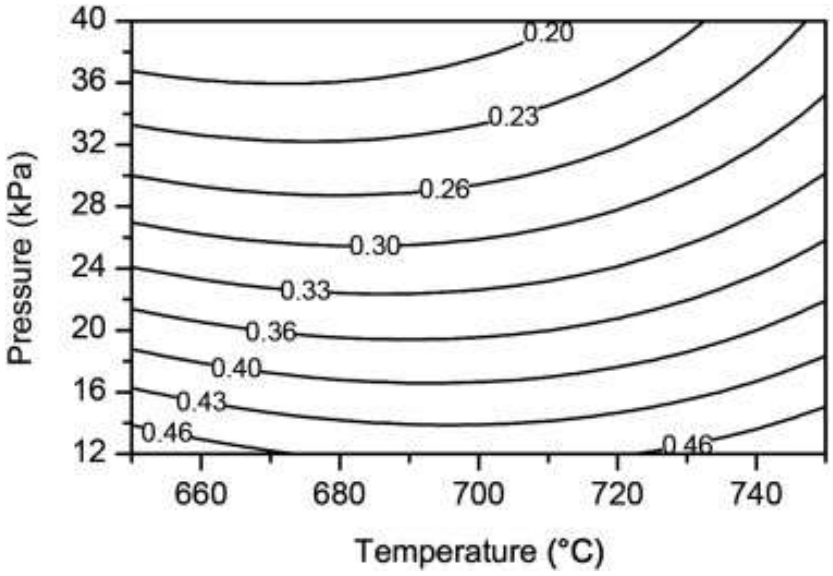

Figure 4 The effect of temperature and pressure on the TFE mole fraction as determined by Meissner [6] in the second section of the horizontal reactor. The contour plot was generated using the response surface equations of Meissner [6] for TFE (Y_7).

Statistical analysis of the octafluorocyclobutane yield

In contrast to the predictions made by Meissner [6], in this system, the OFCB concentration was highly dependent on the operating pressure, as indicated by the density of the contours in Figure 5.

The OFCB concentration was not affected by the interaction variable, therefore, the variable was removed. This did not affect the adjusted R^2 value negatively, as seen in Table 5, supporting the conclusion that the interaction variable is statistically insignificant. By examining the actual measured OFCB mole fraction points in Figure 5, it is clear that the contour plot provides a relatively accurate prediction of the expected OFCB mole fraction. The predicted mole fractions at 750 °C are not as accurate, however, it still does provide a fairly good prediction.

$$Y_3 = 0.2853 + 0.0259X_1 + 0.2544X_2 + 0.0508X_1^2 - 0.0601X_2^2 \quad (16)$$

Table 5: Regression analysis comparison for the OFCB response surface.

	Initial regression analysis with $\beta_3 X_1 X_2$ included	**Regression analysis with $\beta_3 X_1 X_2$ excluded**
R^2	0.956	0.956
Adjusted R^2	0.945	0.947
Significance F	1.55e-13	1.55e-14
Standard error	0.045	0.044

Considering Figure 5, the optimum operating conditions for OFCB would be 750 °C and 40 kPa. Maximum OFCB fractions of 0.5 – 0.55 were observed at operating temperatures of 650 °C – 750 °C and a pressure of 40 kPa. These fractions were almost double than those achieved by both Meissner [6] (see Figure 6 and Figure 7) and van der Walt [2].

The results in Figure 5 indicate that the OFCB concentration is more sensitive to changes in pressure and that the concentration increases with an increase in pressure and temperature. These results are almost the

opposite of those predicted by Meissner [6]. This difference could be attributed to residence time and is discussed further in section 4.4.

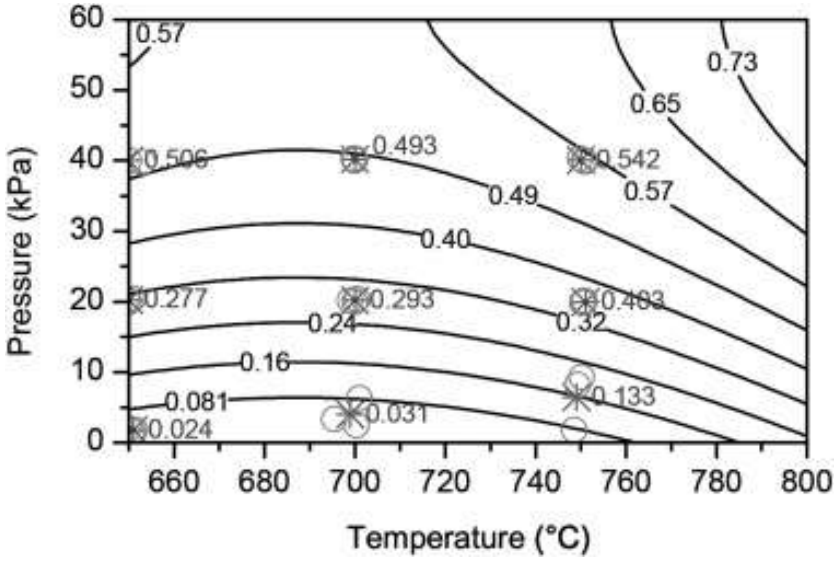

Figure 5 The contour plot of the influence of temperature and pressure on the fractional distribution of OFCB as calculated using equation 16. Data validation was achieved by including the actual experimental data points (O) and the averages calculated for each set which is denoted by a star.

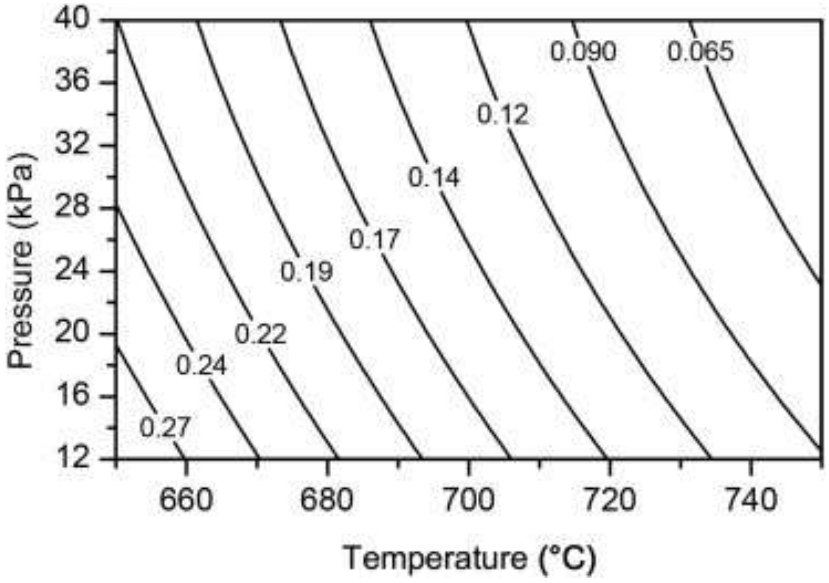

Figure 6 The effect of temperature and pressure on the OFCB mole fraction as determined by Meissner [6] in the first section of the horizontal reactor. The contour plot was generated using the response surface equations of Meissner [6] for OFCB (Y_4).

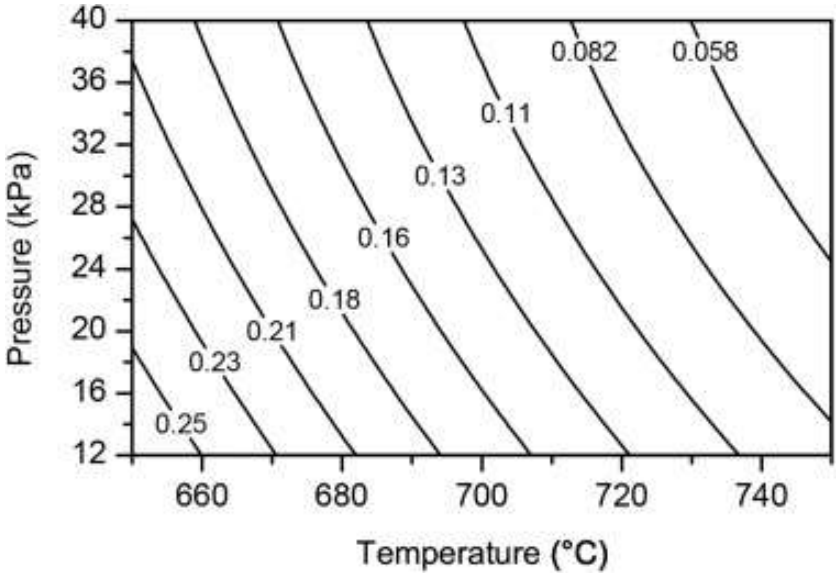

Figure 7 The effect of temperature and pressure on the OFCB mole fraction as determined by Meissner [6] in the second section of the horizontal reactor. The contour plot was generated using the response surface equations of Meissner [6] for OFCB (Y_9).

4.2 Statistical analysis of the hexafluoropropylene yield

As with TFE and OFCB, analysis of the regression data indicated that the interaction variable had no statistical significance in the HFP response function (see Table 6). In contrast to the contour plots of TFE and OFCB, the HFP contour plot provides a very accurate prediction of the HFP mole fraction, even at an operating temperature of 750 °C. HFP production was almost equally affected by changes in temperature and pressure. However, Figure 8 indicates that there is a point of inflection, where the HFP production becomes more sensitive to changes in pressure than temperature. The density of the contours below an HFP fraction of 0.13 indicates that the HFP production is much more sensitive to pressure changes in this region. Above the 0.13 fraction contour, this sensitivity swaps around with the HFP production now more influenced by changes in temperature. These results were in line with those produced by van der Walt [2] and Meissner [6].

$$Y_2 = 0.1121 + 0.0314X_1 + 0.0675X_2 + 0.0344X_1^2 - 0.0314X_2^2 \quad (17)$$

Table 6: Regression analysis comparison for the HFP response surface.

	Initial regression analysis with $\beta_3 X_1 X_2$ included	**Regression analysis with $\beta_3 X_1 X_2$ excluded**
R^2	0.795	0.781
Adjusted R^2	0.741	0.742
Significance F	1.34e-06	5.34e-07
Standard error	0.034	0.034

The maximum observed HFP fraction was 25 mol % at operating conditions of 750 °C and 40 kPa, respectively. These operating conditions coincide with those proposed by both Meissner [6] and van der Walt [2]. However, both Meissner [6] and van der Walt [2] achieved much higher concentrations of HFP (> 64 %). The large difference in the HFP concentration measured during this investigation compared to those reported by Meissner [6] and van der Walt [2] could be attributed to residence time and is discussed further in section 4.3.

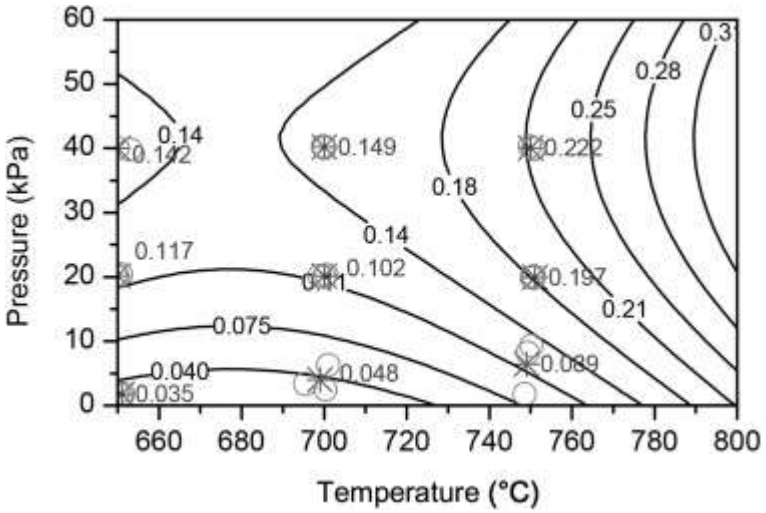

Figure 8 The contour plot of the influence of temperature and pressure on the fractional distribution of HFP as calculated using equation 17. Data validation was achieved by including the actual experimental data points (O) and the averages calculated for each set which is denoted by a star.

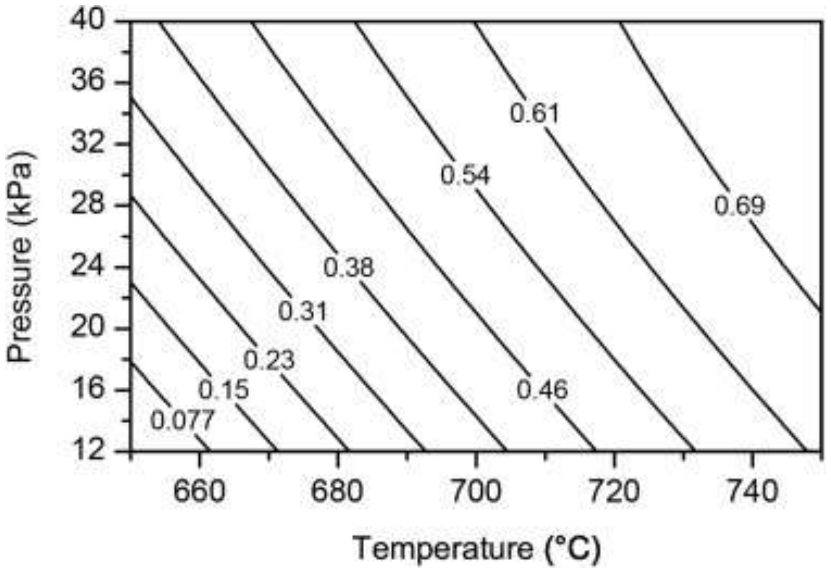

Figure 9 The effect of temperature and pressure on the HFP mole fraction as determined by Meissner [6] in the first section of the horizontal reactor. The contour plot was generated using the response surface equations of Meissner [6] for HFP (Y_3).

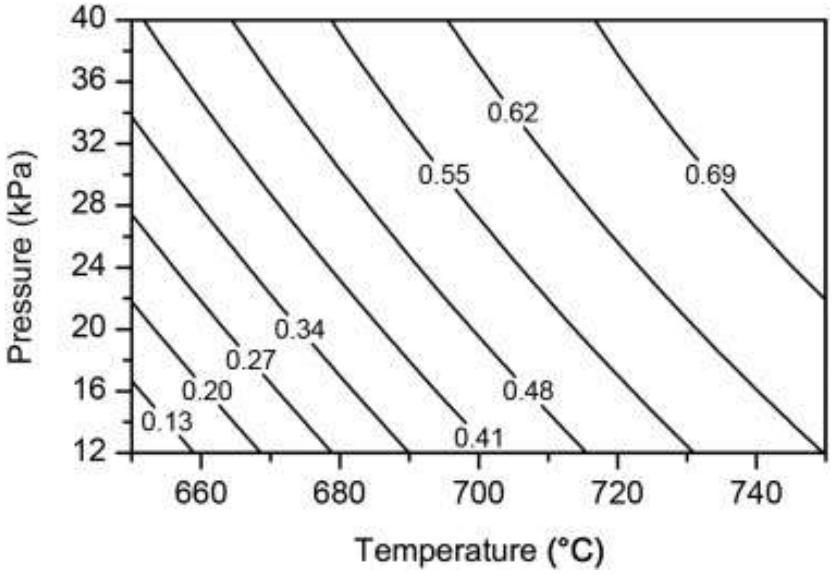

Figure 10 The effect of temperature and pressure on the HFP mole fraction as determined by Meissner [6] in the second section of the horizontal reactor. The contour plot was generated using the response surface equations of Meissner [6] for HFP (Y_8).

4.3 The predicted formation rates of TFE, HFP, and OFCB

The inverted maximum OFCB and HFP concentrations observed by Meissner [6] and van der Walt [2] compared to the maximum concentrations observed during this investigation, could be due to a difference in residence time of the gas products in the reactor. In an effort to investigate the differences in results further; the formation rates of TFE, HFP, and OFCB were predicted using the kinetic data available in the literature. The component specific kinetics (see Table 7) determined by Atkinson [11] for the thermal decomposition of TFE was used to determine the formation of HFP and OFCB. TFE formation was determined by assuming that all of the PTFE is converted to TFE during depolymerisation. It was assumed that this reaction will have the same reaction rate as the overall PTFE depolymerisation rates proposed in the literature. The reaction rates predicted by Siegle [12], Anderson [13], and Conesa [14] for the overall depolymerisation of PTFE are comparable and therefore the average values of the kinetics parameters were used.

The differential equations (equations (21) to (24)) were derived from the total system differential equations (equations (26) to (30)) to take into account that no accurate and reliable kinetic data for reactions (5) and (20) is available in the literature. The derivation was performed by assuming that a steady state is achieved where the difluorocarbene radical concentration remains constant and rate constant k_5 is very small compared to k_3 and k_4, as proposed and derived by Atkinson [11].

Table 7: The OFCB and HFP formation kinetics determined by Atkinson [11] and the averaged PTFE depolymerisation kinetics.

Rate constant symbol	Reaction	Pre-exponential factor		Activation energy (kJ·mol^{-1})	
k_{PTFE}	$PTFE \rightarrow CF_2 = CF_2$	1.5x10^{21}	s^{-1}	339.66	(18)
k_1	$2CF_2 = CF_2 \rightarrow OFCB$	10.3x10^{7}	mol^{-1}·s^{-1}	106.27	(4)
k_2	$OFCB \rightarrow 2CF_2 = CF_2$	8.9x10^{15}	s^{-1}	310.03	(19)
k_3	$OFCB \rightarrow CF_3 — CF = CF_2 + \bullet\bullet\, CF_2$	3.9x10^{16}	s^{-1}	330.50	(6)
k_4	$CF_2 = CF_2 + \bullet\bullet\, CF_2 \rightarrow CF_3 - CF = CF_2$	-	-	-	(5)
k_5	$CF_3 - CF = CF_2 \rightarrow CF_2 = CF_2 + \bullet\bullet\, CF_2$	-	-	-	(20)

$$\frac{dW_{PTFE}}{dt} = -k_{PTFE}W_{PTFE} \quad (21)$$

$$\frac{dN_{TFE}}{dt} = -k_1 N_{TFE}^2 + 2k_2 N_{OFCB} - k_3 N_{OFCB} + \frac{k_{PTFE}W_{PTFE}}{100.02} \quad (22)$$

$$\frac{dN_{OFCB}}{dt} = 0.5k_1 N_{TFE}^2 - k_2 N_{OFCB} - k_3 N_{OFCB} \quad (23)$$

$$\frac{dN_{HFP}}{dt} = 2k_3 N_{OFCB} \quad (24)$$

The predicted reaction rates in Figure 11, follow the same trend as the experimental data except for the HFP fractions. With an increase in reaction temperature, the deviations between the predicted and actual mole fractions measured increase dramatically (see Figure 12 and Figure 13). These deviations could be due to the numerous assumptions made to estimate the residence time, the fact that the product specific kinetics were determined from the pyrolysis of TFE; and the fact that the system was modelled as a plug flow reactor (PFR). The system would more likely resemble a combination between a PFR and a continuous stirred tank reactor (CSTR). Nevertheless, the kinetics do indicate that at an extended residence time the HFP concentration will ultimately increase to above that of TFE and OFCB. The deviations, especially the HFP fractions, can also be explained due to the differential equations not accounting for the production of difluorocarbenes directly from PTFE, as described by reactions (1) and (2); and by assuming

the reaction constant k_5 is small enough to be negligible. It is also assumed that the production of HFP is only from the dissociation of OFCB. Atkinson [11] proposed that the main formation pathway of HFP is through OFCB dissociation. However, this reaction cannot account for the HFP concentrations measured at residence times of 0.2 s and 2.7 s. At these residence times, the OFCB concentration is not high enough to enable reaction (6) to produce these fractions of HFP. Therefore, the HFP concentrations measured at residence times lower than 3 s should mainly be from TFE reacting with difluorocarbenes. Hence, it can be deduced that at low residence times (< 3 s) the main route of HFP production is through reaction (5). With an increase in residence time, the dominant HFP formation pathway shifts to reaction (6). This could explain the clear inflection point observed in the response surface of HFP (Figure 8). With an increase in pressure and temperature, reaction (5) becomes less dominant and at the inflection point reaction (6) becomes the dominant formation pathway for HFP.

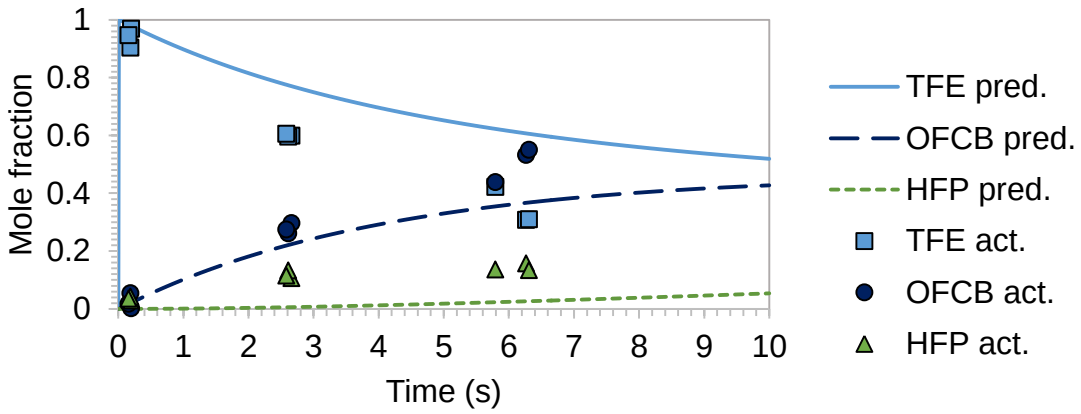

Figure 11 The actual measured mole fractions of TFE, HFP, and OFCB and the predicted mole fractions determined via the differential equations as a function of residence time for a reaction temperature of 650 °C.

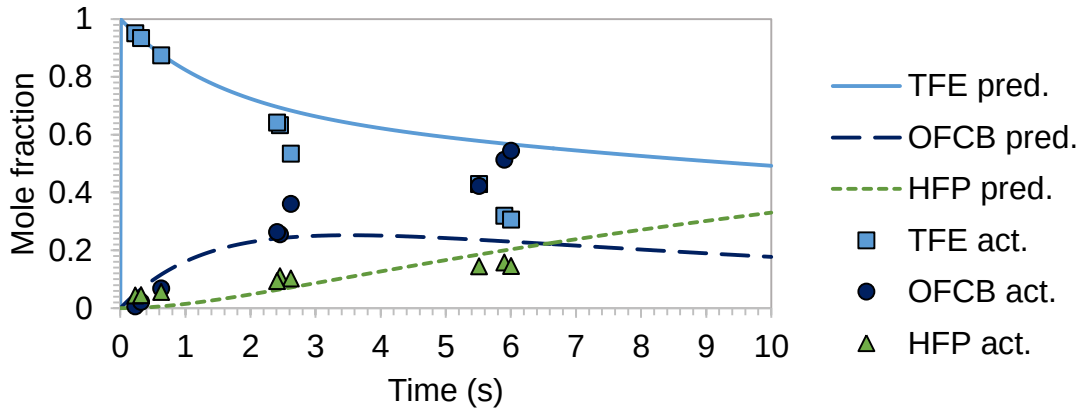

Figure 12 The actual measured mole fractions of TFE, HFP, and OFCB and the predicted mole fractions determined via the differential equations as a function of residence time for a reaction temperature of 700 °C.

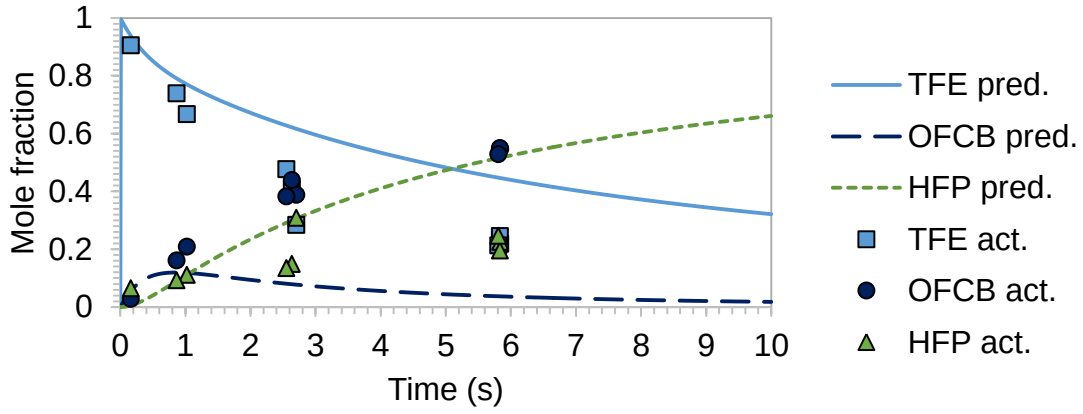

Figure 13 The actual measured mole fractions of TFE, HFP, and OFCB and the predicted mole fractions determined via the differential equations as a function of residence time for a reaction temperature of 750 °C.

The results provided by Meissner [6] and van der Walt [2] had higher concentrations of HFP and lower concentrations of OFCB compared to the results presented in this investigation. This could be explained by the predicted formation rates in Figure 11, Figure 12, and Figure 13. In the depolymerisation experiments of Meissner [6], PTFE was first pyrolysed in a vertical reactor (520 °C and 13.33 kPa – 101.32 kPa), similar to the reactor used in this investigation. The product gas

was then subjected to a second and third heated section in a horizontal reactor where the gas was heated further (600 °C – 800 °C). The residence time and reactor temperature in the vertical reactor in addition to the residence time and increased temperature in the first section of the horizontal reactor could have caused the products to react further. Therefore, leading to higher HFP mole fractions and lower OFCB fractions than reported in this investigation. This same reason could explain why the contour plots (see sections 4.1, 0, and 0) of TFE, HFP, and OFCB differ from those presented by Meissner [6].

These results show that higher HFP concentrations can be achieved if the residence time of the gas in the reactor is increased. The residence time can be increased in two ways: either by increasing the operating pressure or by increasing the reactor volume. However, both of these options could lead to the increased production of PFIB.

4.4 Determination of the product specific kinetics from the experimental data

The product specific kinetics of the system were investigated to study the effects of reactions (5), (6), and (20) on the production of HFP. In section 4.3, it was assumed that the reaction rate of reaction (5) is equal to that of reaction (6) and that the rate of reaction (20) is small enough to be neglected, as proposed by Atkinson [11]. It was also assumed that the main and only pathway of HFP production was through the dissociation of OFCB. It was also assumed that all of the difluorocarbenes produced during PTFE depolymerisation, combines to produce TFE.

To determine the product specific kinetics the reaction equations in Table 8 were assumed. In the table, reaction (25) is the overall reaction that includes reactions (1) and (2), where PTFE depolymerises to produces difluorocarbenes during the initiation step. It was assumed that this reaction will have the same

reaction rate as the overall PTFE depolymerisation kinetics determined in the literature and that all of the PTFE fed in one second (0.183 g·s^{-1}) is converted to difluorocarbenes. The differential equations (equations (26) – (30)) were derived assuming that the reactions in Table 8 are all elementary. In contrast to the differential equations used in section 4.3, reaction (20) was not assumed to be negligible. The product specific kinetics were determined via solving the differential equations in GNU Octave [15]. The reaction rate constants were adjusted until the predicted formation rates of TFE, HFP, and OFCB fit the experimental data in Table 3. The pre-exponential constants and activation energies were determined by plotting $\ln k_i$ as a function of $\frac{1}{T}$. The depolymerisation system was modelled as a Plug Flow Reactor (PFR).

Table 8: The reaction equations used to determine the product specific kinetics for this system.

Rate constant symbol	Reaction	Rate constant units	
k_1	$PTFE \rightarrow \bullet\bullet CF_2$	s^{-1}	(25)
k_2	$2 \bullet\bullet CF_2 \rightarrow CF_2 = CF_2$	mol^{-1}·s^{-1}	(3)
k_3	$2CF_2 = CF_2 \rightarrow OFCB$	mol^{-1}·s^{-1}	(4)
k_4	$OFCB \rightarrow 2CF_2 = CF_2$	s^{-1}	(19)
k_5	$OFCB \rightarrow CF_3{-}CF = CF_2 + \bullet\bullet CF_2$	s^{-1}	(6)
k_6	$CF_2 = CF_2 + \bullet\bullet CF_2 \rightarrow CF_3 - CF = CF_2$	s^{-1}	(5)
k_7	$CF_3 - CF = CF_2 \rightarrow CF_2 = CF_2 + \bullet\bullet CF_2$	s^{-1}	(20)

$$\frac{dW_{PTFE}}{dt} = -k_1 W_{PTFE} \quad (26)$$

$$\frac{dN_{TFE}}{dt} = 0.5k_2 N_{CF_2}^2 - k_3 N_{TFE}^2 + 2k_4 N_{OFCB} - k_6 N_{TFE} N_{CF_2} + k_7 N_{HFP} \quad (27)$$

$$\frac{dN_{OFCB}}{dt} = 0.5k_3 N_{TFE}^2 - k_4 N_{OFCB} - k_5 N_{OFCB} \quad (28)$$

$$\frac{dN_{HFP}}{dt} = k_5 N_{OFCB} + k_6 N_{TFE} N_{CF_2} - k_7 N_{HFP} \quad (29)$$

$$\frac{dN_{CF_2}}{dt} = \frac{k_1 W_{PTFE}}{50} - k_2 N_{CF_2}^2 + k_5 N_{OFCB} - k_6 N_{TFE} N_{CF_2} + k_7 N_{HFP} \quad (30)$$

The formation rates determined for each of the reaction temperatures (650 °C, 700 °C, and 750 °C) are indicated in Figure 14, Figure 15, and Figure 16, respectively. The

determined pre-exponential constant and activation energy for each of the reactions are summarised in Table 9.

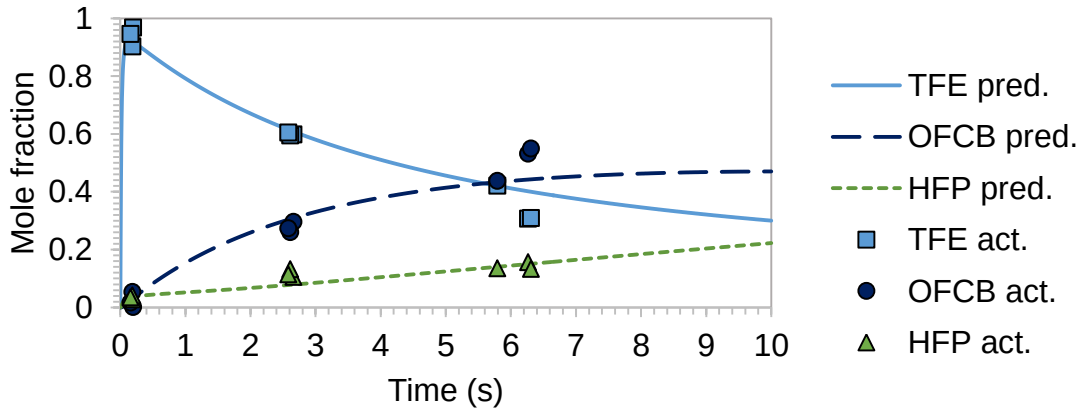

Figure 14 The determined formation rates of TFE, HFP, and OFCB over time compared to the actual product fractions at a temperature of 650 °C.

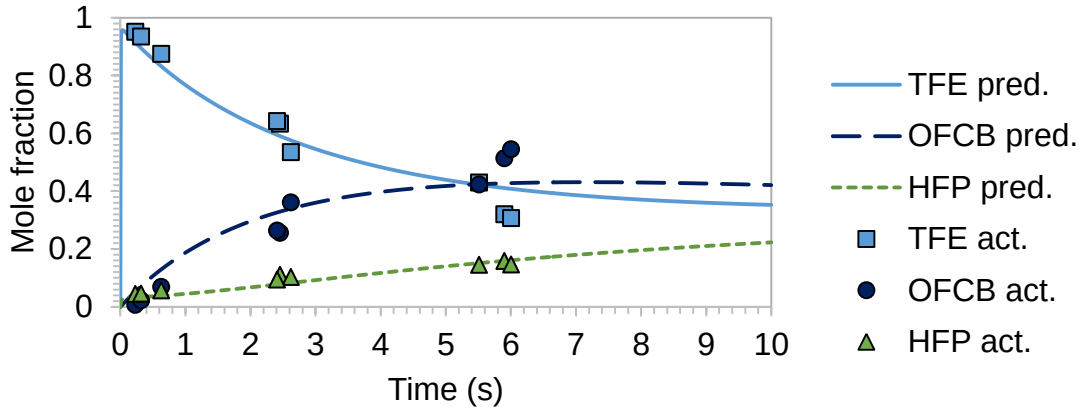

Figure 15 The determined formation rates of TFE, HFP, and OFCB over time compared to the actual product fractions at a temperature of 700 °C.

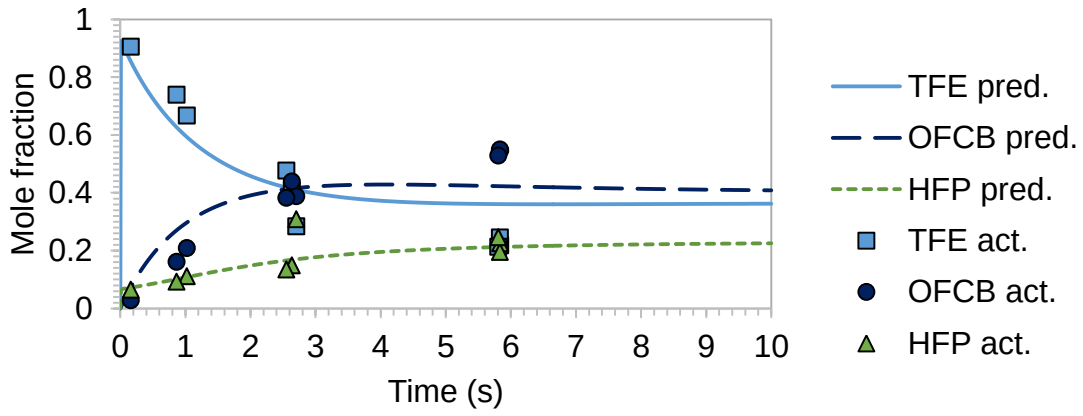

Figure 16 The determined formation rates of TFE, HFP, and OFCB over time compared to the actual product fractions at a temperature of 750 °C.

Table 9: The calculated activation energies and pre-exponential constants for each of the reactions in Table 8.

	Rate constant						
	k_1 s^{-1}	k_2 $mol^{-1}\cdot s^{-1}$	k_3 $mol^{-1}\cdot s^{-1}$	k_4 s^{-1}	k_5 s^{-1}	k_6 s^{-1}	k_7 s^{-1}
Pre-exponent	1.47×10^{21}	3.2×10^{17}	6.28×10^{6}	2.74×10^{15}	1.7×10^{2}	5.11×10^{18}	1.25×10^{22}
Activation energy ($kJ\cdot mol^{-1}$)	339.39	214.25	79	323.79	66.43	274.91	436.01

A comparison of the pre-exponential constants of the various reactions in Table 9 indicate that the reaction rate of reaction (20) (k_7) is not small enough to be neglected, as assumed in the previous section. The data also indicates that the reaction rates of reactions (5) and (6) (k_6 *and* k_5 in Table 9) cannot be assumed to be equal as assumed in the previous section. Atkinson [11] proposed that the main formation pathway of HFP is through OFCB dissociation. However, this reaction cannot account for the HFP concentrations measured at residence times of 0.2 s and 2.7 s. At these residence times, the OFCB concentration is not high enough to enable reaction (6) to produce these fractions of HFP. Therefore, the HFP concentrations measured at residence times lower than 3 s should mainly be from TFE reacting with

difluorocarbenes. Hence, it can be deduced that at low residence times (< 3 s) the main route of HFP production is through reaction (5). With an increase in residence time, the dominant HFP formation pathway shifts to reaction (6).

The calculated kinetics for reactions (4) and (19) (k_3 and k_4 in Table 9) are in line with the data proposed by Atkinson [11]. The pre-exponential constant and activation energy of reaction (6) (k_5) do not correspond with the data proposed by Atkinson [11]; however, they determined the kinetic data from the pyrolysis of TFE and assumed that all of the HFP is produce via OFCB dissociation. They did not account for the production of HFP via reaction (5).

The formation rates in Figure 14, Figure 15, and Figure 16, slightly deviate from the actual mole fraction data points. This could be due to the system being modelled as a PFR. By modelling the system as a PFR, the continuous addition of PTFE into the reactor and the effects thereof on product formation are neglected. Therefore, it is recommended to model the system in future as a PFR/CSTR system to account for these effects. The deviation could also be attributed to the assumptions made in calculating the residence times or the error in determining the mole fractions via the FTIR analysis method. Improving the FTIR calibration for the system and including a flow meter in the system should improve the accuracy of the product specific kinetics.

5 Conclusions

Statistical analysis of the TFE response function indicates that the production of TFE is highly sensitive to changes in pressure. An increase in pressure leads to lower fractions of TFE. This, however, is the complete opposite for the production of HFP and OFCB. An increase in both temperature and pressure leads to higher concentrations of HFP and OFCB. The production of OFCB is highly sensitive to pressure; whereas the formation of HFP is equally affected by pressure and temperature changes.

However, changes in pressure have a larger effect on the HFP production than the temperature at pressures lower than approximately 20 kPa. At higher pressures, the sensitivity switches around with changes in temperature having a larger effect. The statistical result of HFP and OFCB completely contradict the results determined by Meissner [6].

The highest mole fraction of OFCB (0.55) was observed at operating conditions of 40 kPa and 750 °C. Compared to the literature, this is the highest concentration of OFCB achieved at these operating conditions, with both van der Walt [2] and Meissner [6] only achieving a maximum of 0.25. In contrast to the data of both Meissner [6] and van der Walt [2], the maximum observed HFP mole fraction was 0.25 during this investigation. The inverted maximum OFCB and HFP concentrations observed by Meissner [6] and van der Walt [2] compared to the maximum concentrations observed during this investigation, could be due to a difference in residence time of the gas products in the reactor. A brief kinetic analysis of the system, using the relevant kinetic data available in the literature, confirms that the HFP concentration will increase with an increase in residence time.

TFE mole fractions of 0.95 and higher can be achieved with operating temperatures in the range of 650 °C to 720 °C, together with a system pressure of 2 kPa or less. A mole fraction of 0.19 and higher can be expected for HFP within the operating range of 744 °C to 750 °C and 32 kPa up to 40 kPa. To maximise this fraction (> 0.20), without changing the residence time, an operating temperature and pressure of 750 °C and 40 kPa are recommended. However, at these conditions, the OFCB fraction would be maximised at 0.5 or higher. Hence, these conditions would not be optimal if distillation is to be used to separate the mixture. In future, if the need arises to produce a product gas containing mostly TFE and OFCB with an HFP concentration less than 10 mol %, an operating temperature range of 660 °C –

695 °C and operating pressure range of 14 kPa – 20 kPa is recommended. At these conditions, a TFE concentration of ± 65 mol %, an OFCB concentration of ± 25 mol %, and an HFP concentration of ± 9 mol % can be expected.

Analysis of the product specific kinetics indicates that OFCB dissociation is the dominant HFP production pathway only at residence times higher than 3 s. At lower residence times the dominant HFP production pathway is through the reaction of TFE with difluorocarbenes. It was concluded that to increase the HFP concentration and decrease the OFCB concentration, the residence time of the gas in the reactor should be increased. This can be achieved via two methods: either increase the reaction pressure or increase the reactor heated section volume.

Acknowledgement

The study was supported by funding from the National Research Foundation (NRF) and the Fluoro-expansion Initiative (FEI) which is supported by the South African Department of Science and Technology (DST).

References

1. Simon CM, Kaminsky W. Chemical recycling of polytetrafluoroethylene by pyrolysis. Polym Degrad Stab 1998; 62: 1 – 7.

2. Van der Walt IJ, Bruinsma OSL. Depolymerisation of clean unfilled PTFE waste in a continuous process. J Appl Polym Sci 2006; 102: 2752 – 2759.

3. Lewis EE, Naylor MA. Pyrolysis of polytetrafluoroethylene. J Am Chem Soc 1947; 68: 1968 – 1970.

4. Hercules DA, DesMarteau DD, Fernandes RE, Clark JL Jr., Thrasher JS. In: Smith DW, Lacono

ST, Lyer SS, editors. Handbook of Fluoropolymer Science and Technology: Evolution of Academic Barricades for the use of Tetrafluoroethylene (TFE) in the Preparation of Fluoropolymers. NJ, USA: John Wiley & Sons, 2014. p. 413 – 431.

5. Schottle T, Hintzer K, Staudt HJ, Weber H. Process for the preparation of fluorinated monomers. US Patent 5432259, 1995.

6. Meissner E, Wroblewska A, Milchert E. Technological parameters of pyrolysis of waste polytetrafluoroethylene. Polym Degrad Stab 2004; 83: 163 – 172.

7. Ichida T, Homoto Y. (2008) Process for producing fluoromonomer. US Patent 7317071B2, 2008.

8. Morisaki S. Simultaneous thermogravimetry-mass spectrometry and pyrolysis-gas chromatography of fluorocarbon polymers. Thermochim Acta 1978; 25: 171 – 183.

9. Eilers A. A perfect smoother. Analytical Chem 2003; 75(14): 3631 – 3636.

10. Drobny JG. Technology of Fluoropolymers, Second Edition, Florida USA: CRC Press, Taylor & Francis Group, 2009. p. 9.

11. Atkinson B, Atkinson VA. The thermal decomposition of tetrafluoroethylene. J Chem Soc 1957: 2086 – 2094.

12. Siegle JC, Muus LT, Lin T, Larsen, HA. The molecular structure of perfluorocarbon polymers.

II. Pyrolysis of polytetrafluoroethylene. J Polym Sci 1964; 2: 391 – 404.

13. Anderson, HC. Thermogravimetry of polymer pyrolysis kinetics. J of Polym Science 1964; 6: 175 – 182.

14. Conesa JA, Font R. Polytetrafluoroethylene decomposition in air and nitrogen. Polym Eng Sci 2001; 41(12): 2137 – 2147.

15. Eaton JW, Bateman D, Hauberg S, Wehbring R. GNU Octave A high-level interactive language for numerical computations. Free Software Foundation, Boston USA, 2016.